Paper accepted

ENERGY

Thermo-economic analyses of a Taiwanese combined CHP system fuelled with syngas from rice husk gasification

C.T. Chang
Department of Environmental Engineering
National Ilan University of Taiwan, Taiwan
ctchang@niu.edu.tw

M. Costa
Istituto Motori – CNR, Naples, Italy
m.costa@im.cnr.it

M. La Villetta
CMD Costruzioni Motori Diesel
maurizio.lavilletta@cmdengine.com

A. Macaluso
Department of Engineering
University of Naples "Parthenope", Naples, Italy
adriano.macaluso@uniparthenope.it

D. Piazzullo*
Istituto Motori – CNR, Naples, Italy
daniele.piazzullo@students.uniroma2.eu

L. Vanoli
Department of Industrial Engineering
University of Cassino and South Latium, Cassino, Italy
vanoli@unicas.it

ABSTRACT

A Combined Heat and Power (CHP) system fuelled with rice husk is analysed from the thermodynamic, exergetic and economic point of view. The system is based on a gasification process coupled with a rice drying system. The produced syngas is employed to power a Spark Ignition (SI) Internal Combustion Engine (ICE) working as an electric generator, while the jacket cooling water powers a bottoming Organic Rankine Cycle (ORC) to produce electricity for plant self-consumption.

A parametric analysis is carried out to investigate thermodynamic performances by varying the gasifier Equivalent Ratio (ER): as the ER increases, the ICE produced power and combustion efficiency decrease, while the thermal efficiency increases. However, the system is always capable to produce power for self-consumption and the desiccant flow for drying.

The characterization of the engine is then better assessed by means of a dedicated GT-Power engine model, optimized for syngas fuelling, revealing a power derating of the 30% with respect to the natural-gas feeding operation.

Other main findings suggest that the global exergetic efficiency ranges between 10.6% and 8.5%, while the economic profitability, represented by the Simple Pay Back, Net Present Value and Profit Ratio, cannot be considered satisfactory due to the consistent investment cost.

KEYWORDS

Biomass, Gasification, Internal Combustion Engine, Organic Rankine Cycle, Drying, CHP

NOMENCLATURE

Acronyms

AF	Annuity Factor	[-]
BFB	Bubbling Fluidized Bed	
CFB	Circulating Fluidized Bed	
CHP	Combined Heat and Power	
CCHP	Combined Cooling, Heat and Power	
cp	specific heat,	[kJ/kg K], [kJ, kmol K]
daf	dry ash free basis	
db	dry basis	
ER	Equivalent Ratio	
EFGT	Externally Fired Gas Turbine	
$\dot{E}x$	Exergy flow	[kW]
ex	specific exergy	[kJ/kg], [kJ/kmol]
FC	Fixed Carbon	[%]
$\dot{F}_{ex}$	Exergy fuel	[kW]
HE	Heat Exchanger	
HHV	Higher Heating Value	[MJ/kg]
HPR	Heat to Power Ratio	
ICE	Internal Combustion Engine	
IRR	Internal Rate of Return	[-]
LHV	Lower Heating Value	[MJ/kg]
NPV	Net Present Value	[€]
O&M	Operational and Maintenance	
ORC	Organic Rankine Cycle	
PHR	Power to Heat Ratio	
PR	Profit Ratio	[-]
PTC	Parabolic Through Collector	
$\dot{P}_{ex}$	Exergy product	[kW]
$\dot{P}$	Power	[kW]
$\dot{R}_{ex}$	Exergy residual	[kW]

RDF	Refuse Derived Fuel	
SPB	Simple Pay Back	[years]
TES	Thermal Energy Storage	
VM	Volatile Matter	[%]
U	Overall heat transfer coefficient	[kW/m^2 K]
VCC	Vapour Compressor Cycle	
WHR	Waste Heat Recovery	
wt	weight	[%]

Latin letters

a	interest rate	[-]
A	heat transfer area	[m^2]
A	ash content	[%]
C	annual operational cost, specific cost	[€]
C	Carbon	[%]
H	Hydrogen	[%]
J	investment costs	[€]
$\dot{m}$	mass flow rate	[kg/s]
N	Nitrogen	[%]
N	lifetime	[years]
n	moles	[kmol]
$\dot{n}$	molar flow rate	[kmol/s]
O	Oxygen	[%]
P	exergy product	[kW]
p	pressure	[bar]
R	yearly revenue	[€]
R	universal gas constant	[kJ/kmol K]
$\bar{R}$	specific gas constant	[kJ/kg K]
S	Sulphur	[%]
T	absolute temperature	[K]
t	temperature	[°C]
x	molar fraction	
y	mass fraction	
w	water	

Greek symbols

η	efficiency

Subscript

0	dead state
air	air
ash	ashes
av	avoided
CC	combustion chamber
ch	chemical
cool	cooling
des	desiccant flow
destr	destroyed

disp	disposal
el	electric, electricity
ex	exergy, exergetic
exh	exhaust gases
gas	gasifier
HE	Heat Exchanger
Hot	hot
husk	husk
ICE	Internal Combustion Engine
in	inlet
nat,gas	natural gas
net	net
O&M	Operational and Maintenance
ORC	Organic Rankine Cycle
out	outlet
ph	physical
purch.	purchase
ricehusk	rice husk
sell.	selling
st	standard
tot	total
th.	thermal
w	water

1. INTRODUCTION

The last few years have been characterized by a great interest on Combined Heat and Power (CHP) plants fuelled with biomass. This technology is emerging on the market with promising prospects for the near future, such as residue biomass utilization in district heating & cooling and/or in industrial or commercial activities.

CHP systems with low price and easy-to-use operation for industrial and residential end-users are still under development. Future introduction for domestic/commercial applications will depend on the available technologies, on the capability to achieve the requested electrical and thermal loads and on the gas and electricity prices. These economic and technical uncertainties curb the diffusion of micro and small CHP plants, especially in countries where economic incentives are lack or not yet provided for bio-energy production. However authors argue that, CHP plants able to use residual biomass as fuel in specific contexts such as small and medium-sized enterprises, municipalities, farms, sawmills, etc., can be economically sustainable even incentive mechanisms are lack or not yet provided. In fact, residual biomasses that present disposal cost such as biomass from forest harvesting, biomass from communal green areas (such as roadside greenery, greenery along railways, cemeteries, driftwood, heath areas, residues from vegetable gardening, field vegetable residues etc.), food residues (such as chestnuts, almond, hazelnuts, walnut, pistachio, peach, olive kernel, etc.), agricultural biomasses (such as rice husk, etc.) exhausted olive cake, properly pre-treated, sawmill by-products (such as sawdust, wood chips, slabs and splinters), wood shavings, carpenters, can instead be used as raw material in order to produce electrical and thermal energy for the same process.

In this contest, a suitable solution is represented by the exploitation of these residual materials to generate fuels to be used in Internal Combustion Engines (ICEs), where the utilization of biofuels appears as the most intuitive practice **[1, 2]**, including biodiesel **[3]** and specific blends **[4]**. Thermo-chemical conversion through gasification for synthetic gas (or syngas) production is considered as one of the most suitable technology for small scale CHP systems based on the ICE technology **[5**, **6**, **7]**.

ICEs also offer a great potential of Waste Heat Recovery (WHR) [8], since 30 - 40% of the thermal energy fuel content is available at low temperature (80 - 90 °C) in the cooling circuit while about the 30% is available at high temperature (300 - 400 °C) from the exhaust gases **[8]**.

The disadvantages characterizing this technology (low temperature of most of the recoverable heat, low Heat-to-Power Ratio (HPR), noxious emissions and high maintenance costs) are perfectly compensated by a large commercial availability in terms of nominal power, high electric efficiency (35 - 45%), low investment costs, good off-design operation, easiness of integration with other energy sources and technologies in polygeneration systems [**9**, **10**]. Main typical thermodynamic characteristics of such systems are summarized in Table 1 **[11]**.

An interesting example is given in ref. **[12]**, where authors modelled a CHP system based on an ICE co-fired by natural gas and syngas. The waste heat from the ICE is exploited for producing both hot water and chilled water by means of a double effect absorption chiller. The prefeasibility analysis shows a first law efficiency of about 70.0% and an exergy efficiency of 21.9%.

Table 1. Main thermodynamic characteristics of gasifier coupled with ICE fuelled with biomass **[11]**.

Thermodynamic characteristics	**Gasifiers + ICE**
Specific biomass consumption (humidity 40 %) [kg/kWh$_{el}$]	1.2-1.7
Electric efficiency % [-]	~ 25
Thermal efficiency % [-]	~ 45
Heat temperature available [°C]	80-500
Operation time [h/y]	7000
Specific Cost [€/kWe]	3000-5000

Regarding small-scale gasification, a compact cogeneration system producing electricity and cold/hot water (at 65 and 70 °C respectively) is analysed in **[13]** from an energetic and economic point of view. The prime mover is an ICE (15 kW$_{el}$ of power output) fed with wooden gas obtained from a small-sized bed downdraft gasifier. WHR is performed by exploiting both the jacket cooling water and the exhaust gases. The plant is characterized by a global energy efficiency equal to 51.2%, with an electric efficiency equal to 21.4%, and a hot and cold-water generation efficiency equal to 24.3% and 5.71% respectively.

The application of small-scale gasification in the residential field is also studied in [14], applied to buildings configurations characterized by different energetic demands. In this context, this solution appears not suitable due to the variability of users' energy loads, as such technology needs to operate in a continuous mode without any off-design or on/off operation (e.g. as in district heating networks, where users are multiple and loads variability is mitigated with respect to a single building configuration).

In the perspective of WHR purposes from ICE, Organic Rankine Cycle (ORC) is a smart solution to further recover low-grade waste heat energy [15, 16], as for example from the engine cooling circuit. ORC systems consist of a classical Rankine cycle operating with an organic fluid, that, despite some disadvantages (toxicity, flammability and high cost), guarantees attractive properties such as low critical temperature, high latent heat of evaporation and high molecular weight **[17]**. Moreover, it is characterized by easy construction and installation, reliability, easy maintenance, cost-effectiveness **[18]** and easy integration with other technologies **[19**, **20]** in integrated polygeneration plants system **[21]**. For these reasons, it can be considered one of the best technologies to exploit low-medium temperature thermal cascades **[22, 23]** and low-medium enthalpy renewable energies, including geothermal one **[24-26]** and biomass **[27, 28]**. Moreover, application can be multiple, such as domestic **[29]** and district heating **[30]**. In fact, considering manufacturer data [31, 32] latest plants installations all over the world [33, 34], modern ORC modules can operate at heat source temperatures ranging between 80 – 300 °C **[35, 36]**, with a First Law efficiency ranging between 5 - 30 % and a Second Law efficiency in the range 20 - 54 % **[37-39]**. Among the multiple working fluids suitable for ORCs, for low temperature applications the most common ones are Pentane, n-Pentane, Siloxane, R134a and R245fa, which is more suitable for temperature up to 160 °C **[40, 41]**.

Nowadays, the use of ORC technology for WHR from ICE has been widely investigated, both in residential applications [42-44] and in the automotive sector [45-48]. The electrical output of small-scale ORC systems is in the range of 5.00-200 kW_{el}. Actually, the specific ORC investment costs, ranging between 1.10 k€ and 7.40 k€, strictly depends on the project type (layout complexity, power output) and on the specific thermal resource to be exploited **[49]**.

In ref. **[50]**, authors presented a mathematical model and an optimization procedure of a simple layout system, composed by a small scale ICE coupled with an ORC bottoming cycle fed with the engine exhausts. Under the set constraints, among the available organic working fluids, the R245fa represented the best option, with a first law efficiency of 10% and an exergy efficiency of 30%.

On the basis of such findings, an experimental campaign on this small-scale apparatus, with the ICE running at different engine loads (brake power between 50 and 110 kW), resulted in a quite constant thermodynamic efficiency of 10%, while the exergy efficiency ranged between 19 - 30 % with a direct power of 2.00-2.50 kW **[51]**.

In ref. **[52]**, authors presented interesting analyses of a CHP plant based on a updraft gasifier combined with an external combustion chamber and an ORC module. The gasification products are exploited for drying process and burnt in the external combustion chamber. Flue gases indirectly power the ORC module through thermal oil. As reported by the authors, one of the advantages of such system lies in the possibility of avoiding any cleaning and cooling process of the producer gas as it is directly burnt in the combustion chamber. Other advantages are represented by the possibility to process biomass with high ash content and high moisture.

The syngas obtained has a suitable Lower Heating Value (LHV) equal to 4.60 MJ/kg. The ORC module, using Toluene as working fluid, showed an efficiency equal to 18.6%. The CHP layout produced 93.8 kW_{el} of net electric power and 412 kW_{th} of thermal power and it is characterized by 58.4% of first law efficiency.

Another compelling analysis is presented in **[53]**, where authors report a technical assessment of a CHP plant based on a bubbling fluidized bed (BFB) gasifier coupled with an ORC module. The case study is based on real data of a small-scale pilot demonstrator. Main findings suggest that a large-scale system could be sustainable only in the case of fed-in tariffs and of integration into the waste management system. The strength lies in the large amount of landfill space saving and related economic valorisation.

In **[54]**, a very interesting thermodynamic modelling, an economic assessment and comparison of three small-scale power plants layouts based on a downdraft gasifier integrated with an ICE and a ORC bottoming cycle are proposed. In particular, the first configuration is based on the simple ICE-ORC integration presented in **[55]**. In the second configuration, the ORC module is indirectly powered by thermal oil, which is heated in a two-steps phase by the exhaust gases from the ICE and by the hot syngas exiting the fixed bed reactor. Moreover, a preheating process in the ORC cycle through the ICE cooling water is considered. In the third configuration, a double cascade ORC module is proposed, which is composed of two closed loops using two different working fluids: R123 for the topping cycle and R245fa for the bottoming one. Similarly, a preheating process in the bottoming cycle through ICE cooling water is considered.

In the present work, a thermodynamic modelling, an exergetic analysis and an economic assessment of a CHP system designed for a real rice husk dryer system placed in Taiwan are proposed. The layout considered is aimed at maximizing the biomass exploitation for stationary power production, and it was considered within a feasibility study under a specific request of a Taiwanese private company.

The system is composed by a gasification system fed with rice husk. The produced syngas feeds an ICE (topping cycle), whose cooling water powers an ORC module (bottoming cycle). The CHP unit is conceived to be integrated with the rice dryer module, even if the latter is here not simulated.

The power output of the ICE is used for feeding the electricity network, whereas the power output produced by the ORC module is exploited to cover the internal plant demand.

It is to be pointed out that the numerical characterization of the ICE application under biofuel feeding is a challenging task, as the properties of the biofuel resulting from the considered biomass conversion technology deeply affect the combustion efficiency of the primary conversion system. The assessed combustion models, tuned on the ground of a massive amount of experimental data for fossil fuels, often result poor in predicting the actual behaviour under biofuel feeding.

Therefore, the ICE combustion efficiencies under non-conventional fuelling are here analysed through computational modeling on two different levels of detail.

A numerical model of the entire system is first developed within the Thermoflex™ environment, with detailed designing of the heat exchanger performed by using the Exchanger Design & Rating environment of the AspenOne platform. The engine performances are evaluated by resorting to customized Spark Ignition (SI) ICE models available in the software, by studying how the ICE efficiencies vary with the gasifier ER, and consequently, how this influences the system outputs according to users' energetic demand.

The ICE performances are then studied through the development of a more detailed 1D model in GT-Power, optimized according to the composition of the considered gaseous fuel. This study is aimed at better quantifying the engine derating in non-conventional conditions, by comparing the engine performances under a stoichiometric mixture of air and Natural Gas (NG) with the ones relevant to syngas feeding, deriving from rice husk gasification at different values of the gasifier Equivalence Ratio (ER).

Finally, on the basis of the achieved results, an exergetic analysis is proposed, while an economic analysis, aimed at the correct evaluation of the simple payback period is developed, where the economic specific cost functions are considered referring to the Taiwanese market.

2. THE ENERGY SUPPLY AND DEMAND SCENARIO IN TAIWAN: A REVIEW

Taiwan is located in the southeastern rim of Asia, facing the Pacific Ocean in the east and the Taiwan Strait in the west **[56]**. Taiwan is a densely populated island, with a population of over 23.4 million and with only limited natural resources, as over 97% energy supply must depend on oversea imports.

In Taiwan, the total energy consumption has greatly grown over the past two decades, going from 69.18 million kilolitres of oil in 1996 to 116.81 million in 2016.

Classified by energy form, coal contributed to 29.36% in 2016, oil constituted 48.93%, natural gas shared 13.66%, biomass and waste accounted for 1.12%, hydro power provided 0.43%, nuclear power provided 6.25%, solar power, geothermal, wind and biogas power provided 0.17%, and solar thermal the 0.08% (Figure 1.a). Electricity production grew from

142.0 TWh in 1996 to 264.1 TWh in 2016, an average annual increase of 3.15%. Of the total electricity production in 2016, the hydro power of Taiwan Power Company comprised 3.67%, thermal power 52.69% (coal shared 24.71%, oil 3.96%, LNG 24.02%), nuclear power 11.99%, wind power and solar photovoltaic 0.25%, cogeneration 14.56%, and IPP 16.85% (Figure 1.b) **[57]**.

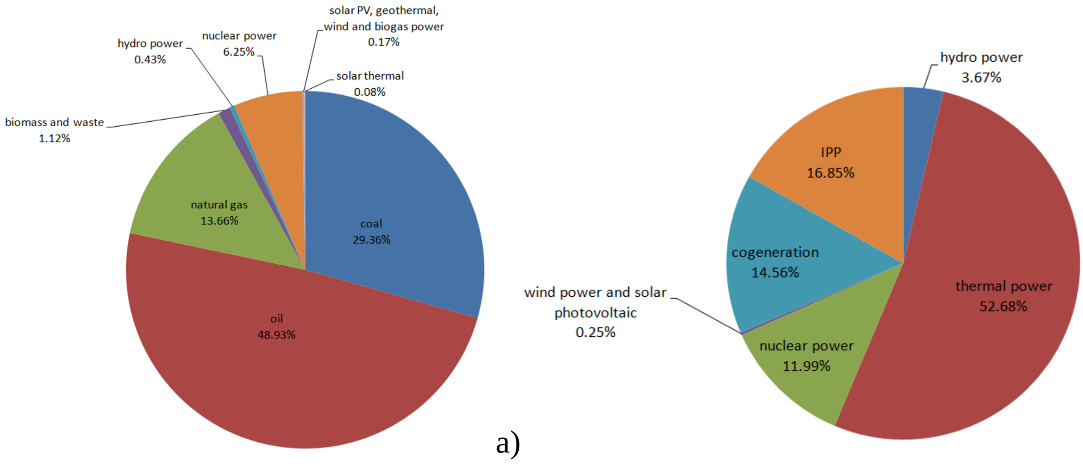

a) b)

Figure 1. a) Classification of energy supply in 2016, b) total electricity production in 2016 **[57]**.

The reserves of renewable energies in Taiwan are 76.48 GW of solar energy, 77.5 GW of wind power, 5.08 GW of biomass, 8.44 GW of ocean energy, 0.7 GW of geothermal and 25.7 GW of hydropower. The total RE reserve is 193.9 GW, which is 4 times of 48.7 GW, the national power capacity in 2015 **[58]**.

As shown in Table 2, the total reserves of biomass energy can be obtained by orderly aggregating the energies from the three categories: first generation of biomass crops, urban waste, and wastes of agriculture and forestry. The reserves of biomass in Taiwan can provide Taiwanese with energy of 38,197.25 GWh/year, equivalent to the electric power of 15,278.90 GWh/year.

Table 2. Assessment of the total reserves of biomass energy in Taiwan **[58]**.

Typology biomass	**Reserves (GW)**	**Equivalent Power (GWh/year)**
Biomass Crops	0.86	3,022.2
Urban waste	1.07	1,208.88
Wastes of Agriculture and Forestry	3.15	1,1047.82
Total Potential	**5.08**	**15,278.90**

The main biomass energy resources are landfill gas and waste incineration, which have total electricity generation capacity of 629.1 MW (at the end of 2015) in more than 70 installed sites. Currently, the installed biomass power is 740 MW in Taiwan, with 625 MW from municipal solid waste incineration, 19 MW from biogas, and 97 MW from waste of industry and agriculture [58]. Nowadays, the most developed current applications that employ biomasses are based on BFB or Circulating Fluidized Bed (CFB) CHP boilers, BFB boilers and Stoker steam boilers, only fuelled with Refuse Derived Fuel (RDF) or with a RDF-coal mix.

In this contest, Taiwanese government is pushing more and more on renewables exploitation, since the island imports the 98.7 % of its energy request **[59]**. Latest Taiwanese approved energy program defines the strategy outlines of renewables and the fee-in tariffs mechanism development. The main goal is targeting the renewables power generation to 17.25 GW at the end of 2030. In particular, target for biomass is fixed at 950 MW **[60]**, with municipal waste exploitation up to 750 MW, industrial waste up to 43 MW, biogas production up to 26 MW and agricultural waste up to 131 MW **[59]**.

3. SYSTEM LAYOUT AND SIMULATION MODELS

The here considered CHP system fuelled with syngas from the gasification of rice husk is analysed within the Thermoflex™ environment, a thermal engineering software usually employed by power and cogeneration industries. Thermoflex™ owns a broad library of working mediums (gases, fuels, refrigerants, etc.) and both pre-built and user-customized commercial power plants, as gas turbines and ICEs. SI engines in Thermoflex™ are supposed to be natural gas fuelled and each pre-built model is characterized by default values of power output, electrical efficiency (hence fuel power input) and flue gas mass flow rate. Therefore, if the engine is fed with a low Lower Heating Value (LHV) fuel instead of methane, and thus a higher mass flow rate of this fluid is required, the software automatically lowers air input to compensate the related increase, keeping the gas mass flow rate constant and always yielding the same power with the same efficiency. This last is a quite strong assumption, as demonstrated by ref. **[61]**. Therefore, in a first step, a customized ICE model in Thermoflex™ is preferred, as it gives the possibility to evaluate the variation of power output with the primary energy content given by the fuel. Indeed, based on the assumption of **[62]**, a certain size ICE is roughly characterized by the same gas mass flow (if the same power output is considered) under both natural gas and syngas feeding. Methane-fed ICEs models in Thermoflex™ can be suitably used to assess the engine performances in case of syngas fuelling.

The considered layout of the here analysed system is shown in Figure 2. Dried biomass and air enter the gasifier; the raw syngas is cleaned through a scrubber and a separator before fuelling the ICE.

The gasifier is based on a thermo-chemical process which converts biomass through partial oxidation into a fuel gaseous mixture (syngas), mainly consisting of H_2, CO, CH_4, CO_2 and N_2.

The syngas needs to be cleaned in order to remove tars and inorganic compounds before being sent to the ICE, whose heat to electric output ratio is typically 2:1.

Before the cleaning, the syngas temperature is decreased (down to 350°C) and the sensible heat transfer in the heat exchanger HE1 is used to warm up the air for the drying section. Since syngas fuel is not enough to heat the air for the drying process of the mass flow rate of rice indicated by the Taiwanese plant owner, another heat exchanger HE2 is employed to recover heat from the exhausts exiting the ICE. Both the HE1 and HE2 are co-axial plate-fin compact heat exchangers. Pressure drop are neglected in both the exchangers.

The ICE cooling circuit is used as hot source in the evaporator of the ORC. R245fa is used as working fluid. Cooling water temperature variation is fixed from 82°C to 92°C. Pressure levels are also fixed at 8 bar for evaporation and 2.5 bar for condensation. The cooling water at the condenser varies between 20°C and 30°C. The generator efficiency is fixed at 95%.

Electricity produced by the ORC module is supposed to be used for self-consumption and cover all the system plants requirements, while the electricity produced by the ICE is sold in the network.

Biomass feeding the gasifier is generally pre-treated by a drying process, aimed at reducing the initial moisture content of the biomass. This pre-treatment increases the conversion efficiency of gasification, leading to a syngas with higher LHV content. However, in this analysis the drying system is not simulated: a fixed desiccant flow rate equal to 450 m^3/min at a minimum temperature of 120 °C is supposed to dry 9000 kg/h of paddy, with an initial moisture content of 26%. This allows feeding the gasifier with a constant mass flow rate of 0.5

kg/s of rice husk biomass, with 15% of moisture content. The operative equivalence ratio of the gasifier is equal to 0.3, as it is a classical condition for gasification. The biomass composition in terms of ultimate and proximate analysis, as derived by the Thermoflex model, is shown in Table 3.

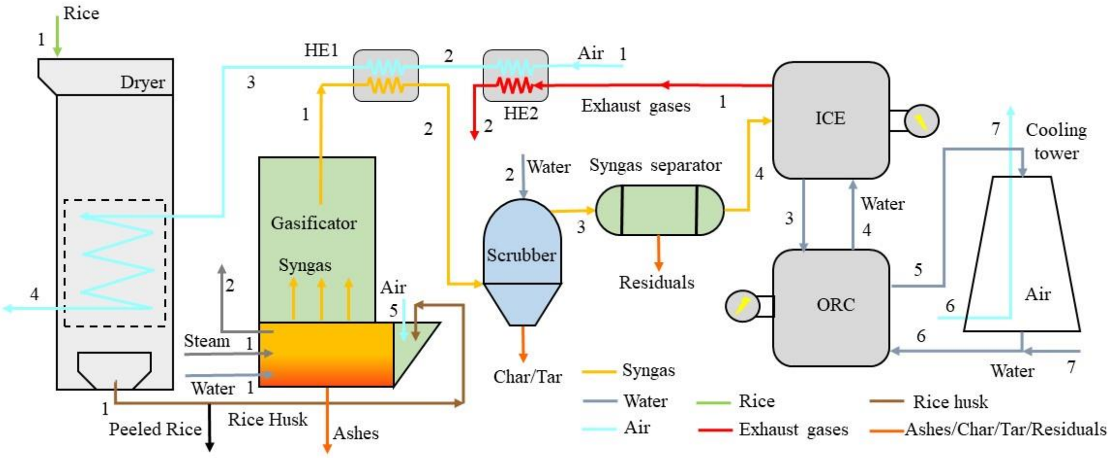

Figure 2. System layout.

Table 3. Biomass ultimate and proximate analysis on dry basis (db) and dry ash free basis (daf).

	db % [w/w]	**daf %[w/w]**
VM (Volatile Matter)	54.4	68.5
FC (Fixed Carbon)	25.0	31.5
Ashes	20.6	
C	31.4	39.6
H	4.76	6.00
O	42.6	53.7
N	0.560	0.700
LHV [MJ/kg]	12.4	15.6
HHV [MJ/kg]	13.4	16.8

The model of the gasifier used for the present layout needs the solid biomass and oxidizing air as input, while the raw syngas composition, temperature of gasification and the slag (this last composed of residual charcoal and ashes) are the main outputs. The reliability of the gasifier model chosen in Thermoflex™ is preliminary assessed considering different initial biomasses, such as rubber wood **[63]**, treated wood **[64]** and sawdust **[65]**, and by comparing the syngas composition with experimental measurements and numerical results obtained using an optimized 0D thermo-chemical equilibrium model **[66]**. Details about the biomass ultimate and proximate analyses may be found in **[66]**, while results of the comparison in terms of species volumetric fraction and gasification temperature are reported in Figure 3. The simulation results in Thermoflex™ refer to full-load steady conditions.

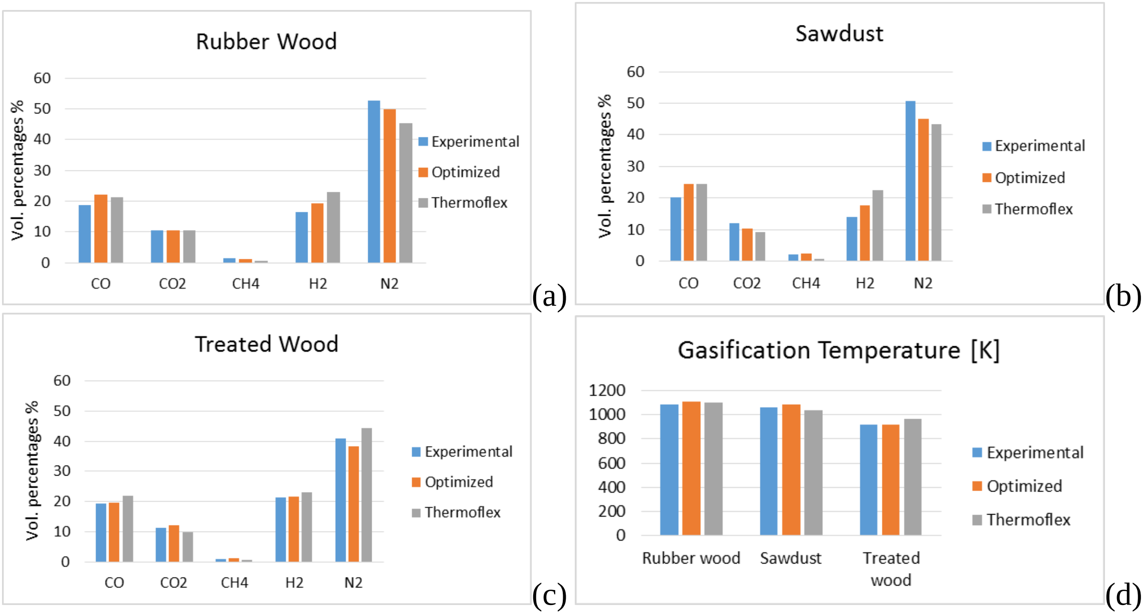

Figure 3. Comparison between experimental measurements, numerical results of both the optimized equilibrium model and the Thermoflex^{TM} model in terms of volumetric syngas compositions for a) rubber wood, b) sawdust, c) treated wood and d) gasification temperature.

3.1. Engine Model and its customization for syngas use

As already said, the definition of the engine operating parameters in the Thermoflex^{TM} environment is performed through the implementation of an engine user-defined configuration, allowing to properly characterise the generation system considered without necessarily having to resort to one of the predefined models present in the vast software library. However, SI ICEs in Thermoflex^{TM} are designed for natural gas combustion, and the evaluation of the performances under syngas fuelling are based on the assumptions that the engine is roughly characterized by the same gas mass flow rate. This assumption, also made by Carrara **[62]**, is based on the hypothesis that the same engine power output is taken into account. Indeed, this goal was fulfilled by feeding the engine with natural-gas under lean burn charge, while syngas combustion occurred under stoichiometric conditions **[62]**.

In the present analysis, a precise evaluation of the engine performances is fundamental to assess how the ICE efficiencies vary with the gasifier ER (thus, with the syngas composition), and how this reflects on the system outputs according to the users' energetic demand.

Therefore, a more detailed analysis of the influence of fuel composition on engine performances can be performed through the development of a dedicated engine numerical model. In this perspective, 1D modelling approaches are a good way to assist the development process of engines, primarily due to their very low computational effort and satisfying accuracy **[67]**. The use of 1D models requires detailed design information of the simulated engine and of the fuel combustion properties and setting-up empirical relations and coefficients to be assessed in a relatively labour-intensive verification with experimental data. In particular, GT-Power **[68]** flow model involves the solution of the Eulerian equations, namely the solution of the equations of conservation of continuity, momentum and energy in one dimension and in the absence of viscosity (ideal case).

As the most of commercial ICEs for stationary energy production are modular configurations, a preliminary analysis is performed to study a single-cylinder engine fuelled with natural gas under stoichiometric charge. The GT-Power model developed is shown in Figure 4: the model is initialized in the *env-inlet-1* component according the initial conditions reported in Table 4, while the geometrical data are specified in the *cylinder1* and *Engine* blocks.

As a first assessment, the length of each intake and exhaust ducts is chosen from the examples available in the software, and properly scaled according to the dimensions of the cylinder.

The predictive turbulent combustion model *EngCylCombSITurb* is chosen to reproduce the combustion occurring under both natural gas and syngas fuelling, since it gives the possibility of evaluating the influence of variation in the composition of the fuel gas.

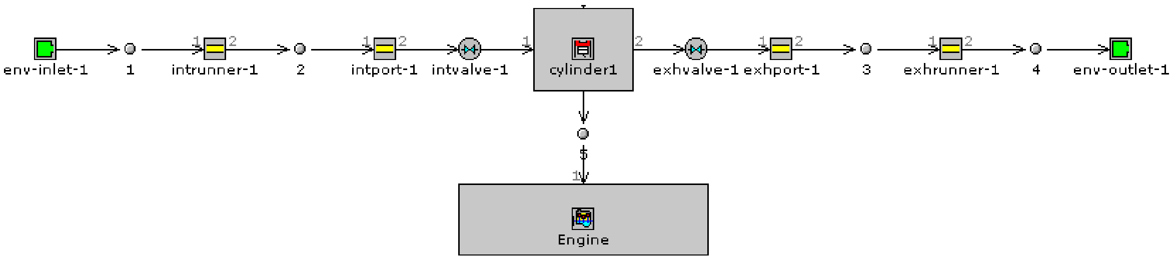

Figure 4. GT-Power model of the JMS 320 GS-C04 single cylinder.

Table 4. Initial conditions considered for the 1D simulation

Mixture	P = 2 bar; T = 313.15 K
RPM	1500
Spark Timing	Between 20° and 5° BTDC
Wall Temperature	Head=550 K; Piston=590 K; Cylinder=450 K

In particular, referring to Eq. 1, the dependency of the laminar flame speed to the combustion parameters is expressed as:

$$S_L = [B_{max} + B_{\varphi} \cdot (\varphi - \varphi_{max})^2] \cdot \left(\frac{T_u}{T_{ref}}\right)^{\alpha} \cdot \left(\frac{p}{p_{ref}}\right)^{\beta} \qquad (1)$$

where B_{max} is the maximum laminar flame speed achieved at the equivalence ratio φ_{max}, B_{φ} is the roll-off value, while α and β indicate the growth/decrease of the laminar flame speed respectively with temperature and pressure. These parameters are set equal to the default values in the case of natural-gas fuelling, while for syngas-fed operations, they are tuned following the approach of Hernandez et al. **[70]**, where validated correlations were obtained according to the producer gas composition and producer gas/air equivalence ratio.

The description of the in-cylinder geometry for the flame and wall interaction is also necessary, while the sub-model chosen to describe the wall heat transfer is the classical Woschni model **[71]** that in the present simulation is used with the default tuning parameters.

Subsequently, a multi-cylinder configuration is taken into account, considering an inline six-cylinder engine analysed under the same operative conditions discussed before. The aim of this study is to quantify the influence on the engine performances of the air pressure pulses that derive from the interaction of all the cylinders. Indeed, the airflow to each cylinder of a multi-cylinder engine, even under steady operating conditions, is not identical. This is due to differences in runner and branch length and other fluid dynamic details of the flow path to each cylinder, and the extent of these with respect to the average flow varies significantly with engine speed and load **[72]**.

Finally, in the last part of the thermodynamic analysis, the engine performances are evaluated under syngas fuelling, obtained from gasification of rice husk under different gasifier equivalence ratio (ER). The results obtained lead to reliable quantifications of the power derating produced by the engine under non-conventional feeding with respect to the previous formulation achieved within Thermoflex™, thus allowing a proper assessment of the exergetic and economic efficiencies of the proposed CHP layout.

4. EXERGETIC ANALYSIS

Since chemical process are involved, particular attention must be paid in the definition and calculation of the exergy of the considered material streams.

In the case of liquid water and neglecting the potential and kinetic energy, the total exergy is only represented by the physical exergy of the material stream.

$$\dot{E}x_{water} = h - h_0 - T_0 \cdot (s - s_0) \tag{2}$$

where h and s are respectively the enthalpy and entropy variations with respect to their value at dead state. As regards the biomass exergy, the simplified formula presented in **[75]**, and reported in Eq. (3) is used.

$$\begin{aligned} ex_{rice\ husk} = {} & 1812.5 + 295.606 \cdot C + 587.354 \cdot H + 17506 \cdot O + \\ & + 17735 \cdot N + 95615 \cdot S - 31.8 \cdot A \end{aligned} \tag{3}$$

where capital letters indicate the content of all the elements expressed in wt%, as db obtained by the ultimate analysis plus the ash content.

Such formula derives by statistical data comparison, which suggest that chemical exergy related to ash and the exergy related to the oxygen reacting with inorganic matter can be neglected. Moreover, authors successfully compare results with the method by Szargut and Styrylska **[76]**, founding a good level of accuracy.

The syngas is considered as a mixture of ideal gases. The total exergy is given by the sum of the physical and chemical contributions.

The complete expression of physical exergy of a gaseous substance, once the thermodynamic parameters T_0 and p_0 at dead state are assessed, is a function of the absolute temperature of the considered stream and of the partial pressure of the ith substance p_i:

$$ex_{ph,i} = c_{p,i} \cdot (T - T_0) - T_0 \cdot c_{p,i} \cdot \ln\frac{T}{T_0} + RT_0 \ln\frac{p_i}{p_0} \tag{4}$$

As shown, global exergy destructions $T_0\Delta S_i$ is given by the sum of the term related to temperature difference and the one related to the mixing effect of each mixture component.

Consequently, the chemical exergy is only given by the standard chemical exergy $ex_{ch,st,i}$.

Finally, the global exergy flux of a gaseous mixture stream is given by the sum of the terms related to each substance:

$$\dot{E}x_{tot} = \dot{n}_{tot} \sum_i x_i \left(ex_{ph,i} + ex_{ch,i}\right) \tag{5}$$

The exergy balances have been written both for all components and for all the system. For the sake of brevity, only the main balances and the efficiency definitions are here reported.

Considering the whole plant, global exergy balance and global efficiency are:

$$\dot{E}x_{rice\,husk} + \dot{E}x_{hot\,air,gas\,in} + \dot{E}x_{des,in} + \dot{E}x_{cool,w,ORC,in} = \dot{P}_{ICE} + \dot{E}x_{des,out} + \\ + \dot{E}x_{cool,w,ORC,out} + \dot{E}x_{exh} + \dot{E}x_{ash} + \dot{E}x_{Char,Tar,Res} + \dot{E}x_{destr} \tag{6}$$

Global exergy efficiency is defined as the ratio between the exergy product and the exergy fuel:

$$\eta_{tot} = \frac{P_{TOT}}{F_{TOT}} = \frac{\dot{P}_{ICE} + \Delta\dot{E}x_{des}}{\dot{E}x_{rice\,husk}} \tag{7}$$

In particular, the exergy product is represented by the sum of the electrical power produced by the ICE and the exergy variation of the desiccant flow, while the exergy fuel is given by the biomass exergy. Exergy related to the hot air entering the gasifier, the exergy related to ashes, char, tar and residual are here neglected.

Considering the main components, namely the gasifier, the ICE and the ORC, the exergy balances and efficiencies are:

Gasifier:

$$\dot{E}x_{rice\,husk} = \dot{E}x_{syn} + \dot{E}x_{destr,gas} \tag{8}$$

$$\eta_{gas} = \frac{P_{gas}}{F_{gas}} = \frac{\dot{E}x_{syn}}{\dot{E}x_{rice\,husk}} \tag{9}$$

ICE^1:

$$\dot{E}x_{syn} + \dot{E}x_{cool,w,ICE,in} = \dot{P}_{ICE} + \dot{E}x_{exh,ICE} + \dot{E}x_{cool,w,ICE,out} + \dot{E}x_{destr,ICE} \tag{10}$$

$$\eta_{ICE,I} = \frac{P_{ICE,I}}{F_{ICE,I}} = \frac{\dot{P}_{ICE}}{\dot{E}x_{ICE}} \tag{11}$$

ICE^2:

$$\dot{E}x_{syn} + \dot{E}x_{cool,w,ICE,in} = \dot{P}_{ICE} + \dot{E}x_{exh,ICE} + \dot{E}x_{des,HE2,out} + \\ + \dot{E}x_{cool,w,ICE,out} + \dot{E}x_{destr,ICE} \tag{12}$$

$$\eta_{ICe,II} = \frac{P_{ICE,II}}{F_{ICE,II}} = \frac{\dot{P}_{ICE} + \Delta\dot{E}x_{des,HE2}}{\dot{E}x_{syn}} \tag{13}$$

ORC:

$$\dot{E}x_{cool,w,ICE,out} + \dot{E}x_{cool,w,ORC,in} = \dot{P}_{ORC} + \dot{E}x_{cool,w,ICE,in} + \dot{E}x_{cool,w,ORC,out} + \\ + \dot{E}x_{destr,ORC} \tag{14}$$

$$\eta_{ORC} = \frac{P_{ORC}}{F_{ORC}} = \frac{\dot{P}_{ORC}}{\dot{E}x_{cool,w,ICE,out} - \dot{E}x_{cool,w,ICE,out}} \tag{15}$$

As shown, two definitions of the exergy balance and efficiency regarding the ICE are reported. In fact, depending on the considered control volume, the definition of the exergy product and of all involved material stream changes.

In the first case, the control volume taken into account is properly the ICE, thus the exergy product is only represented by the power output, while the variation of exergy of the cooling water represents the residual exergy.

In the second case, since the desiccant flow is first heated through the exhaust gases, the considered control volume is the sum of the ICE and the HE2 heat exchanger. Consequently, the exergy product is related both to the power output and to the variation of the desiccant flow at the HE2.

5. ECONOMIC ANALYSIS

The profitability (Eq. 16-24) of the system is assessed by estimating the Simple Pay Back (SPB), the Net Present Value (NPV) and the Profit Ratio (PR).

The SPB is expressed by the ratio between the total investment cost J_{tot} and the sum of operating costs and economic savings, once a traditional biomass butch dryer is considered as reference technology. The total investment cost of the drying retrofitting is trivially given by the sum of the gasifier J_{Gas} **[73]**, of the ICE cost J_{ICE} **[74]**, the ORC cost J_{ORC} **[49]**and the heat exchangers HE1 and HE2, J_{HE} **[75]**. The yearly economic savings are represented by the sum of the revenue $R_{el,sell}$ related to the selling of net electricity supplied ($E_{el,net}$) **[76]**, to the avoided cost of electricity purchase, $R_{el,av.purch.}$ **[76]**, to the avoided cost of thermal energy of the desiccant current $R_{th,av.,}$ and to the avoided cost of rice husk disposal $R_{disp,av}$ (whose specific cost is assessed basing on the information provided by managers and stakeholders operating in this field). The yearly operational costs are given by the Operation&Maintenance costs $C_{O\&M}$ (assumed as the 5.00% of the total investment cost) and by the cost of ash disposal $C_{ash,disp}$ **[77]**.

The NPV is presented by assuming that the total yearly revenue R_{tot} is constant throughout the lifetime of the system (which is set equal to 20 years) and the Interest Rate *a* is equal to 5%.

The PR is calculated as the ratio between the NPV and the total plant investment J_{tot}, as reported in eq. (24)

Parameters used in the analysis are reported in Table

Table 5. Main parameters of the economic analysis.

Input Parameter	**Value**
Specific cost of gasifier C_{Gas}	5000 €/kW
Specific cost of ICE C_{ICE}	1400 €/kW
Specific cost of ORC C_{ORC}	4000 €/kW
Incentive price of electricity (DM 06/2016) C_{sell}	0.14 €/kWh
Purchase price of electricity C_{purch}	0.06 €/kWh
Specific disposal cost of rice husk $C_{disp.husk}$	200 €/ton
Specific cost of natural gas $C_{nat.gas}$ **[78]**	0.400 €/Sm^3
LHV natural gas	34.5 MJ/ Sm^3
Specific disposal cost of ash $C_{disp.ash}$	100 €/ton
Yearly hours of operation	2080 h
Conventional combustion chamber efficiency η_{CC}	97.0%
Interest rate *a*	5.00%
Lifetime *N*	20 years

$$\mathrm{SPB} = \frac{\mathrm{J_{tot}}}{\mathrm{R_{tot}} - \mathrm{C_{tot}}} \tag{16}$$

$$\mathrm{R_{tot}} = \mathrm{R_{el,sell}} + \mathrm{R_{el,av.purch.}} + \mathrm{R_{th.av.}} + \mathrm{R_{disp.av.}} - \mathrm{C_{O\&M}} - \mathrm{C_{ash.disp.}} \tag{17}$$

$$\begin{cases} \mathrm{J_{tot}} = \mathrm{J_{Dry}} + \mathrm{J_{Gas+ICE}} + \mathrm{J_{ORC}} + \mathrm{J_{HE}} \\ \mathrm{J_{Gas+ICE}} = \dot{\mathrm{P}}_{\mathrm{nom.ICE}} \cdot \mathrm{c_{Gas+ICE}} \\ \mathrm{J_{ORC}} = \dot{\mathrm{P}}_{\mathrm{nom.ORC}} \cdot \mathrm{c_{ORC}} \end{cases} \tag{18}$$

$$\mathrm{R_{el,sell}} = \mathrm{E_{el,net}} \cdot \mathrm{c_{sell}} \tag{19}$$

$$\mathrm{R_{el,av.purch.}} = \mathrm{E_{selfcons}} \cdot \mathrm{c_{purch}} \tag{20}$$

$$\begin{cases} \mathrm{R_{disp.av.}} = \mathrm{m_{husk}} \cdot \mathrm{c_{disp.husk}} \\ \mathrm{c_{disp.ash}} = \mathrm{m_{ash}} \cdot \mathrm{c_{disp.ash}} \end{cases} \tag{21}$$

$$\mathrm{AF} = \frac{1}{\mathrm{a}} \times \left(1 - \frac{1}{(1+\mathrm{a})^{\mathrm{N}}}\right) \tag{22}$$

$$\mathrm{NPV} = (\mathrm{R_{tot}} - \mathrm{C_{tot}}) \cdot \mathrm{AF} - |\mathrm{J_{tot}}| \tag{23}$$

$$\mathrm{PR} = \frac{\mathrm{NPV}}{\mathrm{J_{tot}}} \tag{24}$$

6. RESULTS AND DISCUSSION

As discussed in the *Taiwan is located in the* southeastern rim of Asia, facing the Pacific Ocean in the east and the Taiwan Strait in the west **[56]**. Taiwan is a densely populated island, with a population of over 23.4 million and with only limited natural resources, as over 97% energy supply must depend on oversea imports.

In Taiwan, the total energy consumption has greatly grown over the past two decades, going from 69.18 million kilolitres of oil in 1996 to 116.81 million in 2016.

Classified by energy form, coal contributed to 29.36% in 2016, oil constituted 48.93%, natural gas shared 13.66%, biomass and waste accounted for 1.12%, hydro power provided 0.43%, nuclear power provided 6.25%, solar power, geothermal, wind and biogas power provided 0.17%, and solar thermal the 0.08% (Figure 1.a). Electricity production grew from 142.0 TWh in 1996 to 264.1 TWh in 2016, an average annual increase of 3.15%. Of the total electricity production in 2016, the hydro power of Taiwan Power Company comprised 3.67%, thermal power 52.69% (coal shared 24.71%, oil 3.96%, LNG 24.02%), nuclear power 11.99%, wind power and solar photovoltaic 0.25%, cogeneration 14.56%, and IPP 16.85% (Figure 1.b) **[57]**.

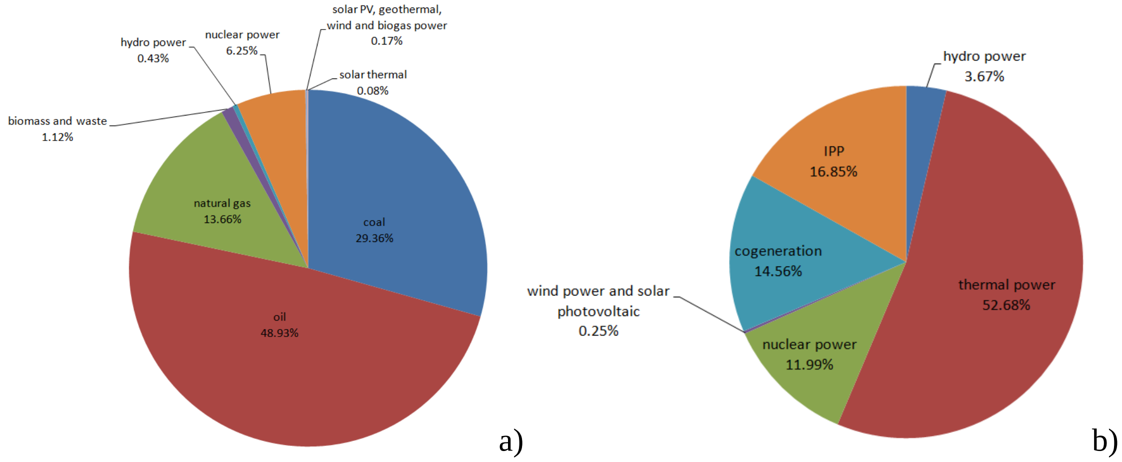

a) b)

Figure 1. a) Classification of energy supply in 2016, b) total electricity production in 2016 **[57]**.

The reserves of renewable energies in Taiwan are 76.48 GW of solar energy, 77.5 GW of wind power, 5.08 GW of biomass, 8.44 GW of ocean energy, 0.7 GW of geothermal and 25.7 GW of hydropower. The total RE reserve is 193.9 GW, which is 4 times of 48.7 GW, the national power capacity in 2015 **[58]**.

As shown in Table 2, the total reserves of biomass energy can be obtained by orderly aggregating the energies from the three categories: first generation of biomass crops, urban waste, and wastes of agriculture and forestry. The reserves of biomass in Taiwan can provide Taiwanese with energy of 38,197.25 GWh/year, equivalent to the electric power of 15,278.90 GWh/year.

Table 2. Assessment of the total reserves of biomass energy in Taiwan **[58]**.

Typology biomass	**Reserves (GW)**	**Equivalent Power (GWh/year)**
Biomass Crops	0.86	3,022.2
Urban waste	1.07	1,208.88
Wastes of Agriculture and Forestry	3.15	1,1047.82
Total Potential	**5.08**	**15,278.90**

The main biomass energy resources are landfill gas and waste incineration, which have total electricity generation capacity of 629.1 MW (at the end of 2015) in more than 70 installed sites. Currently, the installed biomass power is 740 MW in Taiwan, with 625 MW from municipal solid waste incineration, 19 MW from biogas, and 97 MW from waste of industry and agriculture [58]. Nowadays, the most developed current applications that employ biomasses are based on BFB or Circulating Fluidized Bed (CFB) CHP boilers, BFB boilers and Stoker steam boilers, only fuelled with Refuse Derived Fuel (RDF) or with a RDF-coal mix.

In this contest, Taiwanese government is pushing more and more on renewables exploitation, since the island imports the 98.7 % of its energy request **[59]**. Latest Taiwanese approved energy program defines the strategy outlines of renewables and the fee-in tariffs mechanism development. The main goal is targeting the renewables power generation to 17.25 GW at the end of 2030. In particular, target for biomass is fixed at 950 MW **[60]**, with municipal waste exploitation up to 750 MW, industrial waste up to 43 MW, biogas production up to 26 MW and agricultural waste up to 131 MW **[59]**.

SYSTEM LAYOUT AND SIMULATION MODEL*s* section, the reliability of the gasifier model of Thermoflex^{TM} is preliminary assessed by comparing the syngas composition of different biomasses obtained using an optimized 0D thermo-chemical equilibrium model with experimental measurements and numerical results

A cleaning section downstream of the gasifier is generally present in the majority of the real configurations. However, the produced syngas exiting the gasifier is actually modelled as already clean, being composed only by CO, CO_2, CH_4, H_2, N_2 as shown in Table 6. Thus, the devices dedicated to syngas cleaning are considered to evaluate the correct power consumption of the whole system and, in case of scrubbing, determine a syngas moisture variation (which is always completely removed at the end of the treatment chain).

For a gasification ER of 0.3, the ICE power output is 1150 kW_{el} with an electrical efficiency equal to 27.9%. The heat recovery allows the air for the dryer to reach a final temperature of 124 °C. As regards the ORC, it produces 76.3 kW_{el} and it works with a thermal efficiency equal to 6.5% that remains unchanged by varying the ICE power output, since the pressure levels are supposed to be maintained constant, than the specific enthalpy variations are constant and only the mass flow-rate changes.

Table 6. Syngas species composition on daf basis obtained from rice husk gasification, expressed as volume [v/v] and mass [w/w] fractions.

	% [v/v]	**% [w/w]**
CO	22,6	26,8
CO_2	13,8	25,7
H_2	25,6	2,20
CH_4	6.00×10^{-4}	4.00×10^{-4}
N_2	38,1	45,3

A parametric study is proposed with respect to the power output by the engine and the ORC by varying the ER of the gasifier in the range of 0.2 - 0.4, and by keeping constant the biomass flow rate, the dryer air flow rate and the ORC operative parameters. The main results of the parametric analysis are shown in Figure 5.

As the equivalence ratio of the gasifier increases, a reduction of CH_4, H_2 and CO is achieved (Figure 5.a), leading to a reduction of the related syngas LHV and to an increase of the gasification temperature (Figure 5.b), as a consequence of the operative conditions that are approaching the stoichiometric one. This reflects on the useful power of the ICE that reduces due to the lower primary energy content of the syngas, as well as on the thermal energy of the exhaust gases (Figure 6.a). The reduction of the ICE electrical efficiency is accompanied by an increase of the thermal energy content of the exhaust gases (Figure 6.a). The ORC system, working at the same efficiency, produces less electrical power as the gasifier equivalence ratio increases, due to a reduction in the flow rate of the working fluid (Figure 6.b).

Finally, in Figure 6.c the trend of temperatures is reported. The air that is supposed to enter the dryer increases from 83.5 °C to 162.4 °C thanks to the heat transfer that occurs in the two heat exchangers: the increase in the syngas temperature has a stronger effect with respect to the slight reduction that occurs in the exhaust gases energy.

Once the system is analysed by the thermodynamic point of view, a detailed designing of all the heat exchangers is performed in the Exchanger Design&Rating environment of AspenOne platform. Results are reported in Table 7.

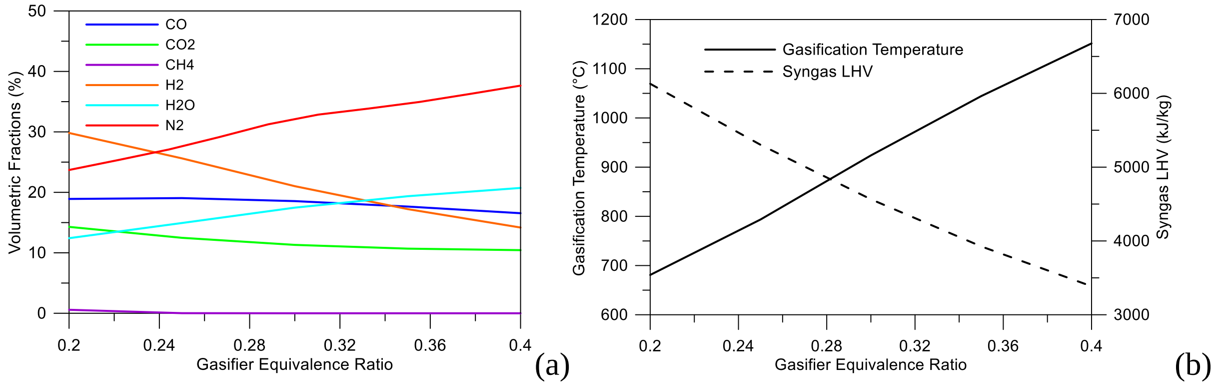

Figure 5. Trends as a function of the gasifier equivalence ratio of a) syngas species composition, b) gasification temperature and syngas LHV.

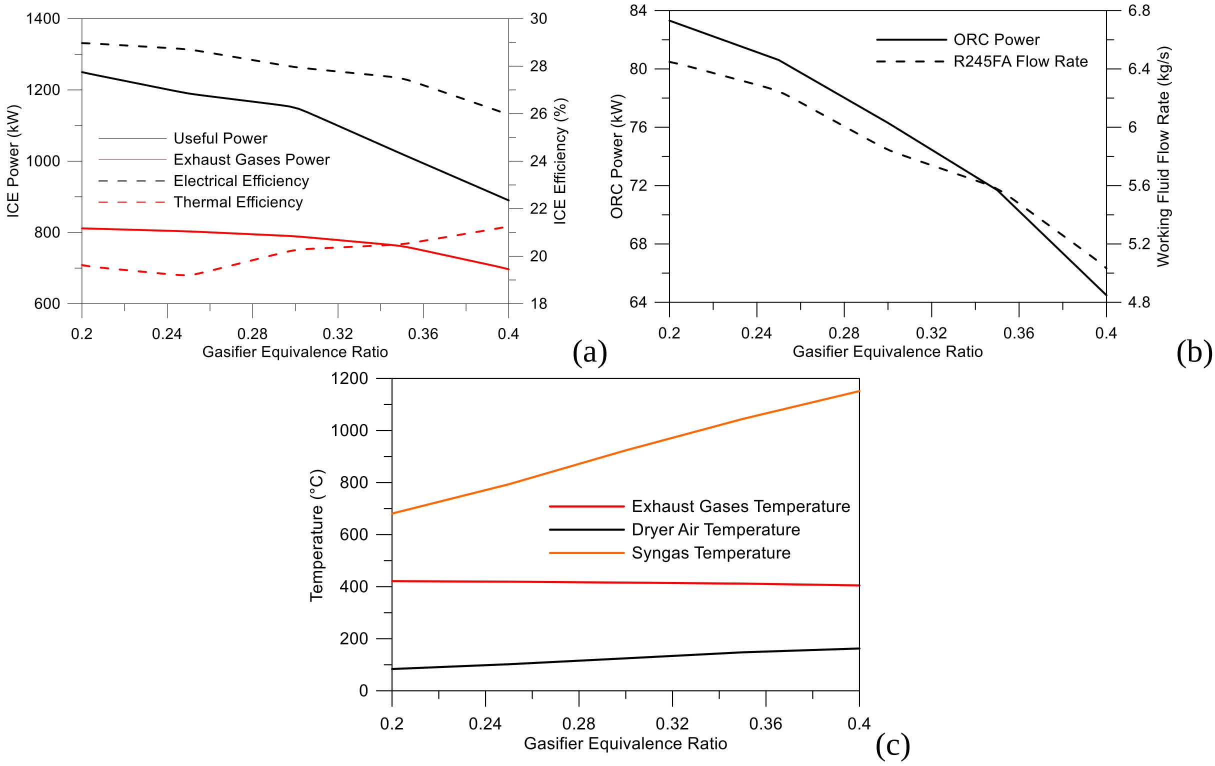

Figure 6. Trends as a function of the gasifier equivalence ratio of a) ICE useful and thermal power, and ICE electrical and thermal efficiency, b) ORC power output and working fluid flow rate, c) exhaust gases, syngas and air dryer temperatures.

Table 7. Design parameters of HE1 and HE2 heat exchangers.

Geometrical feature - Standard axial flow –		
(Gasifier ER=0.3)	**HE1**	**HE2**
UA	1.60 kW/K	0.7 kW/K
Heat transfer area	189 m^2	88.7 m^2
Core length	84.1 cm	210 cm
Core width	114 cm	106 cm
Core depth (stack height)	63.3 cm	60.3cm
No. of layer per exch.	63.0	60.0

6.1. Engine Model Optimization

A more detailed analysis of the influence of fuel composition on engine performances is then performed through the development of a dedicated 1D engine numerical model in GT Power environment.

The characterization of the considered engine is performed by taking information in literature about the engine characteristics, among the natural-gas fuelled systems, whose electrical power is of about 1 MW (according to the results of Figure 6.a). Therefore, a turbo-charged engine JMS 320 GS-C04 **[69]** natural gas fuelled is considered, whose characteristics are reported in Table 8.

The analysis on the engine performances under syngas fuelling lead to quantifications of the power derating with respect to the formulation of the Thermoflex™ environment, thus allowing a more precise assessment of the exergetic and economic efficiencies of the proposed CHP layout.

Table 8. JMS 320 GS-C04 engine characteristics [69].

N° of cylinders	20 V70°
Bore [mm]	135
Stroke [mm]	170
Displacement [dm^3]	48.67
Compression Ratio	12.5
Mean Piston Speed [m/s]	8.5
Electrical Power [kWel]	1063
Recoverable Thermal Power [kWth]	1222
Electrical Efficiency [%]	40.1
Thermal Efficiency [%]	46.1

6.1.1 Single-Cylinder Analysis under Natural Gas Fuelling

The first analysis is focused on an engine mono-cylinder configuration. The results of the parametric study performed by varying the SOS are reported in Figure 7 in terms of brake power expressed in kW. In particular, a SOS equal to 10° BTDC gives a brake power equal to 59 kW. By considering a typical electric efficiency equal to 0.9, this result gives an electric output equal to the target one (being the nominal total power evaluated divided by the number of cylinders). Table 9 reports the main performances of the engine in this last operative condition.

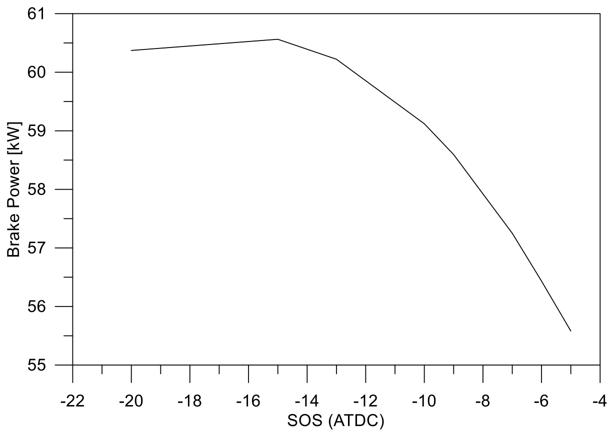

Figure 7. GT-Power result of engine single-cylinder brake power as a function of the SOS under natural gas fuelling.

Table 9. Main results of the single-cylinder simulation at SOS = 10° BTDC under natural gas fuelling.

Indicated Mean Effective Pressure (IMEP) [bar]	21.8
Brake Power [kW]	59
Brake Efficiency [%]	37.52
Exhaust Gases Power [kW]	71.8
Exhaust Gases Efficiency [%]	45.6
Maximum Pressure [bar]	107
Crank Angle at Maximum Pressure [° ATDC]	19.26

6.1.2 Six-Cylinders Analysis under Natural Gas Fuelling

The simulations performed considering a six-cylinder configuration are based on the operative characteristics obtained in the previous section. As previously said, this study is aimed at quantifying the influence on the engine performances of the air pressure pulses that derive from the interaction of all the cylinders, and it is conceived to give a target electrical power of 53 kW.

A parametric study is performed by varying the start of spark (SOS) in a range between 25° and 3° Before Top Dead Centre (BTDC), in order to achieve the produced target power. The firing order chosen is equal to 1-5-3-6-2-4.

Figure 8 shows how, even under the maximum brake torque (MBT) condition (relative to a SOS of 21° BTDC), the brake power is not equal to six times the one produced by the single-cylinder configuration, confirming the effectiveness of the flow interaction on the whole engine performances. This case, whose performance characteristics are reported in ~~Table 40~~ Table 10, is taken into account as reference condition to the evaluation of the variation in engine performances under syngas fuelling.

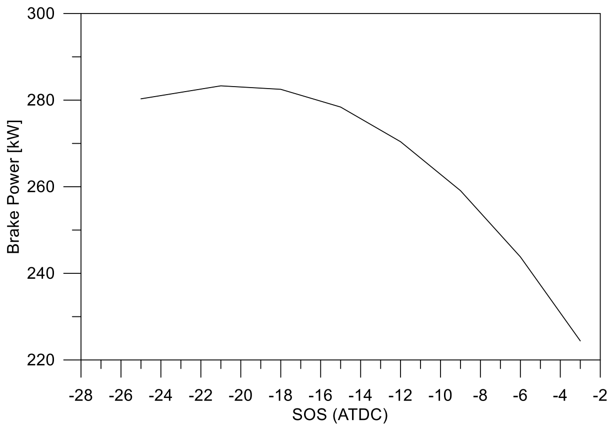

Figure 8. GT-Power result of engine six-cylinder brake power as a function of the SOS under natural gas fuelling.

Table ~~40~~ 10. Main results of the six-cylinder simulation at SOS = 21° BTDC under natural gas fuelling.

Indicated Mean Effective Pressure (IMEP) [bar]	18.6
Brake Power [kW]	283.3
Brake Efficiency [%]	36.4
Exhaust Gases Power [kW]	324.3
Exhaust Gases Efficiency [%]	41.7
Maximum Pressure [bar]	128.6
Crank Angle at Maximum Pressure [° ATDC]	11.6

6.1.3 Six-Cylinders Analysis under Syngas Fuelling

Lastly, the analysis is performed under syngas fuelling in the same operative conditions of the previous section. Table 11 reports the syngas species mass fractions considered for different gasifier ER according to the results of the Thermoflex^{TM} simulation, both with the parameters values of Eq. 1 chosen to correctly describe the laminar flame speed propagation according to the producer gas composition **[72]**.

Table 11. Syngas species mass fractions at different gasifier ER and laminar flame speed parameter.

ER	**0.2**	**0.25**	**0.3**	**0.35**	**0.4**
CO [w/w %]	25.19	24.02	22.98	21.2	19.54
CO_2 [w/w %]	29.80	26.70	21.86	20.20	19.40
H_2 [w/w %]	2.80	2.31	1.86	1.48	1.19
CH_4 [w/w %]	0.53	0.21	0.05	0	0
H_2O [w/w %]	10.51	11.96	13.8	14.7	15.68
N_2 [w/w %]	31.17	34.8	39.51	42.42	44.18
LHV [MJ/kg]	3.67	3.42	3.10	2.85	2.59
B_{max} [m/s]	0.95	0.73	0.57	0.385	0.285
B_{φ} [m/s]	-2.125	-1.58	-1.162	-0.78	-0.419

The results of the present analysis performed at different gasifier ER are reported in ~~Table 52~~ Table 12.

At a fixed SOS, increasing ER leads to a producer gas characterised by a lower primary energy content (lower heating value, as Figure 5.b), thus determining a lower indicated mean effective pressure and brake power produced by the engine. On the other hand, the power related to the thermal energy of the exhaust gases increases with ER.

The trends seen in Figure 6.a for the engine efficiencies are thus confirmed. Nevertheless, the electric efficiency ranges between 18% and 30% (assuming a generator efficiency equal to 0.9), while the thermal efficiency reaches a value equal to 63.8% for ER equal to 0.4. Obviously, each efficiency is related to a syngas primary energy content that varies according to the producer gas deriving from different values of the gasifier ER.

Moreover, Figure 9 reports the evolution of the brake and thermal efficiencies with the SOS for the syngas feeding from different ER.

An interesting result is the shifting of the SOS at which the maximum brake efficiency occurs as the syngas composition varies. Indeed, the reduction in the lower heating value of the gaseous fuel leads to an advancement of the SOS necessary to achieve the maximum exploitable power.

The results of Figure 9 are better highlighted in Figure 10 and Figure 11, where response surface maps are drawn to report the influence of the operative SOS and gasifier ER on the engine power and efficiencies of ~~Table 52~~ Table 12, these lasts expressed as a ratio with respect to the natural gas operative conditions seen in Table 40.

Under syngas fuelling, the engine gives a brake power reduction ranging between the 30.3% and the 64% for an ER respectively equal to 0.2 and 0.4, as a direct consequence of the lower energy content that characterises the syngas fuel with respect to the natural gas (Figure 10.a). On the other hand, it is possible to achieve a 20% higher thermal power of the exhaust gases under syngas fuelling for ER of 0.4 and for advanced SOS (Figure 10.b). Same trends in the engine efficiencies can be derived from Figure 11.

The results here described lead to quantifications of the power derating under non-conventional fuelling. Therefore, the future assessment of the exergetic and economic efficiencies will be performed by taking into account these results of brake power produced, these lasts properly scaled to a 20 cylinders engine.

Table ~~52~~ 12. Main results of the six-cylinder simulation at SOS = 21° BTDC under syngas fuelling.

ER	0.2	0.25	0.3	0.35	0.4
Indicated Mean Effective Pressure (IMEP) [bar]	13.40	12.85	12.32	10.06	7.88
Brake Power [kW]	197.45	186.32	175.36	146.25	101.54
Brake Efficiency [%]	33.19	32.56	31.39	24.8	20.8
Exhaust Gases Power [kW]	244.91	255.65	266.56	289.67	311.86
Exhaust Gases Efficiency [%]	46.59	47.02	47.87	54.24	63.87
Maximum Pressure [bar]	121.37	103.85	87.93	72.59	59.79
Crank Angle at Maximum Pressure [° ATDC]	7.53	8.65	11.65	5.32	0.61

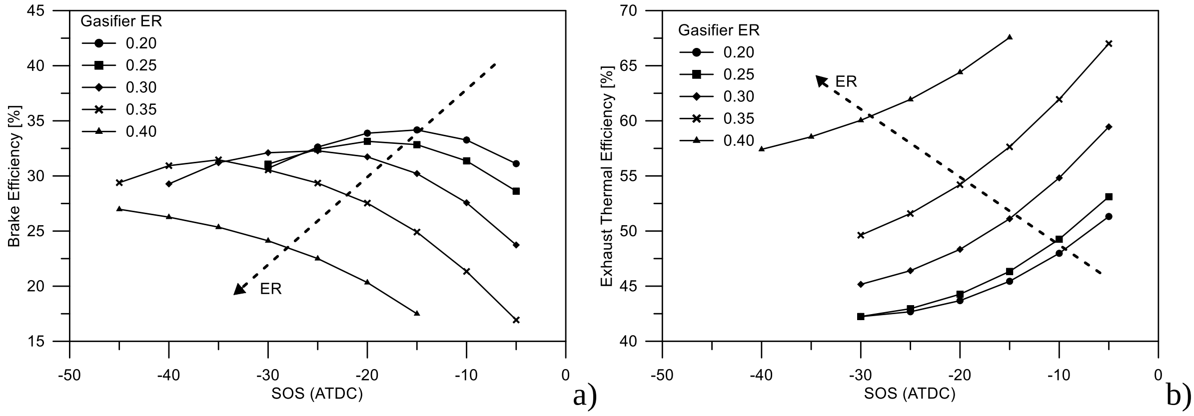

Figure 9. GT-Power result of engine six-cylinder under syngas fuelling of a) brake efficiency and b) exhaust thermal efficiency as a function of gasifier ER and SOS.

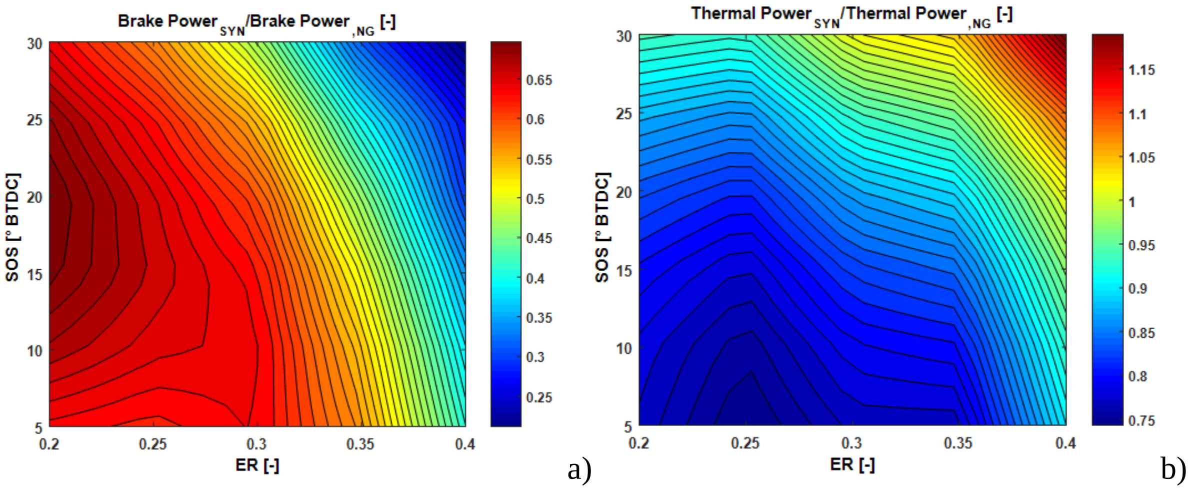

Figure 10. Response surface map of a) brake power and b) exhaust thermal power with respect to the value expressed in Table 10 as a function of gasifier ER and SOS.

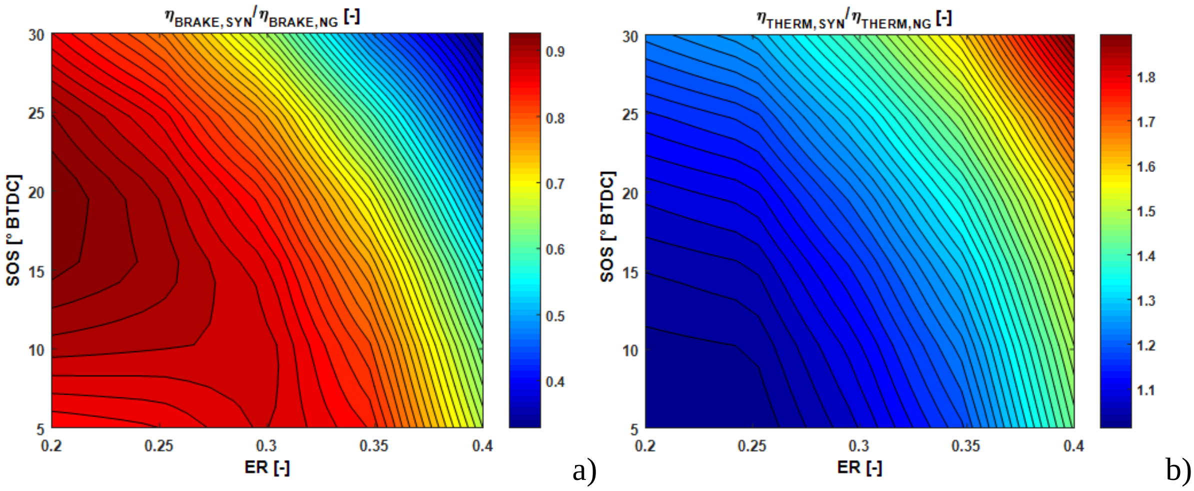

Figure 11. Response surface map of a) brake efficiency and b) exhaust thermal efficiency with respect to the value expressed in Table 10 as a function of gasifier ER and SOS.

6.2 Exergetic analysis

In this section the exergetic analysis of the considered plant layout is reported and discussed.

In ~~Table 63~~ Table 13, main results are shown. The analysis is carried out by varying the gasifier ER from 0.2 to 0.4 with a step of 0.05

Table ~~63~~ 13. Exergetic analysis at different gasifier ER.

ER		**0.2**	**0.25**	**0.3**	**0.35**	**0.4**
$\mathbf{F_{gas}}$	[kW]	6995	6995	**6995**	6995	6995
$\mathbf{P_{gas}}$	[kW]	4743	4659	**4606**	4529	4517
η_{gas}	[%]	67.8%	66.6%	**65.8%**	64.7%	64.6%
$\mathbf{F_{ICE,II}}$	[kW]	4743	4659	**4606**	4529	4517
$\mathbf{P_{ICE,II}}$	[kW]	656.4	619.6	**582.5**	486.8	338.6
$\eta_{ICE,II}$	[%]	13.8%	13.3%	**12.7%**	10.8%	7.50%
$\mathbf{F_{ORC}}$	[kW]	269.1	260.7	**217.0**	232.8	210.1
$\mathbf{P_{ORC}}$	[kW]	83.00	80.00	**76.30**	72.00	65.00
η_{ORC}	[%]	30.84%	30.68%	**35.03%**	30.93%	30.94%
$\mathbf{F_{tot}}$	[kW]	6995	6995	**6995**	6995	6995
$\mathbf{P_{tot}}$	[kW]	710.1	710.0	**737.9**	696.3	595.1
$\mathbf{R_{tot}}$	[kW]	802.2	792.6	**739.6**	758.9	706.6
$\mathbf{\dot{E}x_{destr,tot}}$	[kW]	5483	5493	**5518**	5540	5694
η_{tot}	[%]	**10.2%**	**10.2%**	**10.6%**	**9.95%**	**8.51%**

Results regarding the nominal ER, equal to 0.3, are in bold character. The total exergy of the fuel F_{tot}, represented by the exergetic content of the rice husk, as explained in the simulation model section, amounts to 6995 kW, while the total exergy product P_{tot}, given by the power output of the ICE and by the exergy variation of the desiccant flow, is 737.9 kW. Consequently, the total exergy efficiency of the whole plant η_{tot} amounts to 10.6%. Moreover, the total exergy residual R_{tot}, mainly due to the exergy flow related to the ORC cooling water and to exhaust gases exiting the plant, amounts to 739.6 kW. The total exergy destroyed to 5518 kW. It is worth noticing that the total exergy destruction does not only regard the main component here considered (gasifier, ICE and ORC), but the total plant including the heat exchangers and the component of the syngas cleaning process, namely the scrubber and the separator, which are, from an exergetic point of view, dissipative components.

As regard the parametric analysis, the total exergy of the fuel does not change since the mass flow rate of rice husk and its chemical composition are constant.

Considering the gasifier ER ranging between 0.2 and 0.3, the total exergy produced varies between 710.1 and 737.9 kW, presenting a maximum value for ER equal to 0.3. In fact, the lower production of electricity is balanced by the higher exergy increment of the desiccant current, characterized by a higher outlet temperature thanks to the specific operative conditions of the gasifier.

The total exergy residual varies between 739.6 and 802.2 kW: this is mainly due to the variation of the mass flow rate of the exhaust gases, which presents the lower value at ER equal to 0.4. However, the decrease of residual exergy is compensated by an increase of the total exergy production and of the total exergy destruction (from 5483 to 5518 kW), thus the total exergy efficiency remains quite stable.

Indeed, the global exergy efficiency ranges between 10.2% and 10.6%, with the maximum value at ER equal to 0.3.

Considering the ER ranging between 0.3 and 0.4, as this variable increases the total exergy production decreases from 737.9 to 595.1 kW: this is due to both the lower temperature of the desiccant flow exiting the plant and entering the dryer and the lower electricity production.

Total exergy residuals decrease from 739.6 to 706.6 kW, as well as the total exergy products.

Then the total exergy destructions increase from 5510 to 5694 kW.

The global exergy efficiency presents a more marked variation, ranging from 10.6% to 8.51%.

6.3 Economic analysis

In this section, the economic analysis is presented and discussed.

In ~~Table 74~~ Table 14 the main results are reported. The analysis is carried out by varying the ER from 0.2 to 0.4 with a step of 0.05.

Table ~~74~~ 14. Main results of economic analysis.

			ER				
			0.20	**0.25**	**0.30**	**0.35**	**0.40**
Investment costs	J_{Gas}	M€	5.315	5.315	5.315	5.315	5.315
	J_{ICE}	M€	1.488	1.488	1.488	1.488	1.488
	J_{ORC}	k€	320.0	320.0	320.0	320.0	320.0
	J_{HE}	k€	89.28	89.28	89.28	89.28	89.28
	J_{Tot}	M€	7.212	7.212	7.212	7.212	7.212
Yearly revenues	$R_{el,sell}$	k€	225.4	212.8	200.2	167.0	116.0
	$R_{el,av.purch}$	k€	11.98	11.98	11.98	11.98	11.98
	$R_{th,av}$	k€	36.50	46.36	58.47	70.92	78.82
	$R_{disp,av}$	k€	880.6	880.6	880.6	880.6	880.6
Operational costs	$C_{O\&M}$	k€	360.6	360.6	360.6	360.6	360.6
	$C_{ash,disp}$	k€	8.986	8.986	8.986	8.986	8.986
	C_{Tot}	k€	369.6	369.6	369.6	369.6	369.6
	R_{Tot}	k€	784.8	782.1	**781.7**	760.9	717.8
SPB		years	9.190	9.222	**9.227**	9.479	10.05
NPV		M€	2.568	2.535	**2.529**	2.270	1.733
PR		%	35.61	35.14	**35.06**	31.48	24.03

As shown, the economic performances are only influenced by electricity sales $R_{el,sell}$, whose production is influenced by the operative conditions of the gasifier and the ICE and by the avoided cost of thermal energy $R_{th,av}$; the other variables are kept constant.

In particular, the higher is the ER, the lower is the electricity production (as shown in the thermodynamic analysis) and the related yearly revenue, which monotonically decreases from 225.4 to 116.0 k€.

Conversely, the avoided cost of thermal energy increases as the ~~Er~~ ER increases, ranging from 35.60 to 78.82 k€: this is due to the higher temperature of the desiccant current entering the dryer and then to the higher thermal energy exploitation.

Despite the increment of the avoided cost as the ER increases, the lower electricity production highly affects the total yearly revenue R_{tot}, which monotonically decreases from 784.8 to 717.8 k€.

Consequently, all the calculated economic indices, namely the SPB, the NVP and the PR get worse as the ER increases. In fact, the SPB increases from 9.19 to 10.0 years and the NPV decreases from 2.57 to 1.73 M€, which correspond a PR equal to 35.6% and to 24.0% respectively.

Considering a plausible upper limit for the SPB equal to 5-6 years, the SPB obtained from the analysis is considerably higher. Similarly, considering a plausible lower limit for the PR equal to 50-60%, the PR came out from the analysis appears too low.

Therefore, the economic performances of the analysed system cannot be considered satisfactory because of the higher investment costs needed for the dryer retrofitting.

Finally, it is worth noticing that the best operating conditions from a thermodynamic and exergetic point of view, obtained for ER equal to 0.3, do not correspond to the operating conditions that ensure the best economic performances, that are relevant to ER equal to 0.2.

CONCLUSIONS

A CHP system based on the thermochemical exploitation of rice husk is analysed from a thermodynamic and economic point of view. The main power unit consists of an ICE fuelled with syngas deriving from the biomass gasification, producing electricity to be sent in the network. Moreover, ICE cooling water is exploited to fuel a bottoming ORC, whose electricity produced is used for the system self-consumption.

The desiccant current for the rice drying pre-treatment is produced by exploiting in cascade the thermal energy available from the hot syngas and from exhausts.

The system performances are studied through a parametric study performed as a function of the gasifier ER (between 0.2 and 0.4), keeping constant the biomass flow rate, the dryer air flow rate and the ORC operative parameters as imposed by the real rice manufacturer.

As ER increases, the electric efficiency of the ICE reduces, because of the reduction of the related syngas LHV, while the thermal energy content of the exhaust gases increases due to the higher outlet temperature of the exhausts. At nominal condition of ER equal to 0.3, the ICE power output is equal to 1150 kWel with an electrical efficiency equal to 27.9%. The heat recovery allows the air for the dryer to reach a final temperature of 124 °C. As regards the ORC, it produces 76.3 kWel and it works with a thermal efficiency equal to 6.5%. The desiccant current entering the dryer increases from 83.5 °C to 162.4 °C.

The ICE power derating under non-conventional feeding (syngas fuelling) is then better assessed through the development of a more detailed 1D numerical model in GT-Power environment: the engine power reduction ranges between the 30% and the 64% for an ER respectively equal to 0.2 and 0.4. On the other hand, it is possible to achieve a 20% higher thermal power of the exhaust gases under syngas feeding for ER of 0.4 and for advanced SOS. Main findings also reveal an electric efficiency ranging between the 18% and 30% in the ER range studied, while the thermal efficiency reaches a value equal to 63.8% for an ER equal to 0.4.

The exergetic and economic analyses are then carried out by taking into account results from 1D simulations. At nominal operative conditions, the total exergy of fuel, represented by the exergetic content of the rice husk, amounts to 6995 kW. The total exergy product P_{tot}, given by the power output of the ICE and by the exergy variation of the desiccant flow, is 738 kW and the total exergy efficiency of the whole plant η_{tot} amounts to 10.6%. The total exergy residual R_{tot} is mainly related to the ORC cooling water and to exhaust gases exiting the plant and it amounts to 740 kW. The total exergy destroyed amounts to 5518 kW, and it shows a quite stable trend with ER variations.

In summary, the best operating condition from a thermodynamic and exergetic point of view is the one relevant to an ER equal to 0.3, while the best economic performances are obtained for an ER equal to 0.2.

As regards the economic analysis referred to the specific case study, the main findings suggest the economic performances of the system cannot be considered satisfactory because of the high investment costs. Even changing operating conditions, the improvements are quite moderate. However, the study clearly show how use of CHP plant based on gasification process that use residual biomass (possibly in a short chain area of 70 km radius) brings an high avoided cost associated to disposal, realizing additional revenues from electric and thermal production. This aspect, that fit with circular economy concepts, will promote the use of bio-energy systems also when incentive mechanisms are lack or not yet provided or even high investment costs seem discourage the diffusion of the technologies.

ACKNOWLEDGEMENTS

Financial support of the bilateral agreement CNR-MoST Taiwan: WORTH-IT PROJECT "*Waste heat recovery through traditional or Organic Rankine cycle from rice husk incineraTion: a modeling approacH for Increasing The energy efficiency*" is gratefully acknowledged.

Istituto Motori – CNR would like to thank the National Ilan University of Taiwan, Taiwan.

REFERENCES

[1] Carbot-Rojas D, Escobar-Jiménez R, Gómez-Aguilar J, Téllez-Anguiano A. A survey on modeling, biofuels, control and supervision systems applied in internal combustion engines. *Renewable and Sustainable Energy Reviews*. 2017;73:1070-1085

[2] Sadeghinezhad E, Kazi S, Sadeghinejad F, Badarudin A, Mehrali M, Sadri R, et al. A comprehensive literature review of bio-fuel performance in internal combustion engine and relevant costs involvement. *Renewable and Sustainable Energy Reviews*. 2014;30:29-44

[3] Agarwal AK. Biofuels (alcohols and biodiesel) applications as fuels for internal combustion engines. *Progress in energy and combustion science*. 2007;33(3):233-271

[4] Mofijur M, Rasul M, Hyde J, Azad A, Mamat R, Bhuiya M. Role of biofuel and their binary (diesel–biodiesel) and ternary (ethanol–biodiesel–diesel) blends on internal combustion engines emission reduction. *Renewable and Sustainable Energy Reviews*. 2016;53:265-278

[5] Piriou B, Vaitilingom G, Veyssière B, Cuq B, Rouau X. Potential direct use of solid biomass in internal combustion engines. *Progress in Energy and Combustion Science*. 2013;39(1):169-188

[6] Martínez JD, Mahkamov K, Andrade RV, Lora EES. Syngas production in downdraft biomass gasifiers and its application using internal combustion engines. *Renewable Energy*. 2012;38(1):1-9

[7] IRENA. Renewable Energy Tchnologies: Cost Analysis Series. Biomass for Power Generation. Vol.1: Power Sector. Issue: 1/5. (2012).

[8] Saidur R, Rezaei M, Muzammil W, Hassan M, Paria S, Hasanuzzaman M. Technologies to recover exhaust heat from internal combustion engines. *Renewable and sustainable energy reviews*. 2012;16(8):5649-5659

[9] Chandra ST, Kumar HA. Review on utilization of waste heat & renewables fuels in Internal Combustion engine. *Int J Curr res*. 2016;8:26587-26590

[10] Jradi M, Riffat S. Tri-generation systems: Energy policies, prime movers, cooling technologies, configurations and operation strategies. *Renewable and Sustainable Energy Reviews*. 2014;32:396-415

[11] Frigo S, Gabbrielli R, Puccini M, Seggiani M, Vitolo S. Small-scale wood-fuelled chp plants: a comparative evaluation of the available technologies. *Chemical Engineering Transactions*. 2014;37:847-852

[12] **Wang J, Mao T, Sui J, Jin H. Modeling and performance analysis of CCHP (combined** cooling, heating and power) system based on co-firing of natural gas and biomass gasification gas. *Energy*. 2015;93:801-815

[13] Coronado CR, Yoshioka JT, Silveira JL. Electricity, hot water and cold water production from biomass. Energetic and economical analysis of the compact system of cogeneration run with woodgas from a small downdraft gasifier. *Renewable Energy*. 2011;36(6):1861-1868

[14] Prando D, Patuzzi F, Pernigotto G, Gasparella A, Baratieri M. Biomass gasification systems for residential application: an integrated simulation approach. *Applied Thermal Engineering*. 2014;71(1):152-160

[15] Hung T-C, Shai T, Wang SK. A review of organic Rankine cycles (ORCs) for the recovery of low-grade waste heat. *Energy*. 1997;22(7):661-667

[16] Rahbar K, Mahmoud S, Al-Dadah RK, Moazami N, Mirhadizadeh SA. Review of organic Rankine cycle for small-scale applications. *Energy conversion and management*. 2017;134:135-155

[17] Bao J, Zhao L. A review of working fluid and expander selections for organic Rankine cycle. *Renewable and Sustainable Energy Reviews*. 2013;24:325-342

[18] Desideri A, Gusev S, Van den Broek M, Lemort V, Quoilin S. Experimental comparison of organic fluids for low temperature ORC (organic Rankine cycle) systems for waste heat recovery applications. *Energy*. 2016;97:460-469

[19] Bellos E, Tzivanidis C. Parametric analysis and optimization of a solar driven trigeneration system based on ORC and absorption heat pump. *Journal of Cleaner Production*. 2017;161:493-509

[20] Ghaebi H, Farhang B, Parikhani T, Rostamzadeh H. Energy, exergy and exergoeconomic analysis of a cogeneration system for power and hydrogen production purpose based on TRR method and using low grade geothermal source. *Geothermics*. 2018;71:132-145

[21] Calise F, Macaluso A, Piacentino A, Vanoli L. A novel hybrid polygeneration system supplying energy and desalinated water by renewable sources in Pantelleria Island. *Energy*. 2017;137:1086-1106

[22] David G, Michel F, Sanchez L. Waste heat recovery projects using Organic Rankine Cycle technology–Examples of biogas engines and steel mills applications. Conference Waste heat recovery projects using Organic Rankine Cycle technology–Examples of biogas engines and steel mills applications.

[23] Lecompte S, Huisseune H, Van Den Broek M, Vanslambrouck B, De Paepe M. Review of organic Rankine cycle (ORC) architectures for waste heat recovery. *Renewable and Sustainable Energy Reviews*. 2015;47:448-461

[24] Fiaschi D, Manfrida G, Rogai E, Talluri L. Exergoeconomic analysis and comparison between ORC and Kalina cycles to exploit low and medium-high temperature heat from two different geothermal sites. *Energy Conversion and Management*. 2017;154:503-516
[25] Astolfi M, Romano MC, Bombarda P, Macchi E. Binary ORC (organic Rankine cycles) power plants for the exploitation of medium–low temperature geothermal sources–Part A: Thermodynamic optimization. *Energy*. 2014;66:423-434
[26] Astolfi M, Romano MC, Bombarda P, Macchi E. Binary ORC (Organic Rankine Cycles) power plants for the exploitation of medium–low temperature geothermal sources–Part B: Techno-economic optimization. *Energy*. 2014;66:435-446
[27] Andritsos G, Desideri A, Gantiez C, Lemort V, Quoilin S. Steady-state and dynamic modelling of a 1 MWel commercial waste heat recovery ORC power plant. *Steady-state and dynamic modelling of a 1 MWel commercial waste heat recovery ORC power plant*. 2016
[28] Liu H, Shao Y, Li J. A biomass-fired micro-scale CHP system with organic Rankine cycle (ORC)–Thermodynamic modelling studies. *Biomass and Bioenergy*. 2011;35(9):3985-3994
[29] Qiu G, Shao Y, Li J, Liu H, Riffat SB. Experimental investigation of a biomass-fired ORC-based micro-CHP for domestic applications. *Fuel*. 2012;96:374-382
[30] Prando D, Renzi M, Gasparella A, Baratieri M. Monitoring of the energy performance of a district heating CHP plant based on biomass boiler and ORC generator. *Applied Thermal Engineering*. 2015;79:98-107
[31] TURBODEN. Available at: www.turboden.com. Last access: November 28th. 2017
[32] ENOGIA. Available at: www.enogia.com. Last access: November 28th. 2017
[33] Bertani R. Geothermal power generation in the world 2005–2010 update report. *geothermics*. 2012;41:1-29
[34] Tchanche BF, Lambrinos G, Frangoudakis A, Papadakis G. Low-grade heat conversion into power using organic Rankine cycles–A review of various applications. *Renewable and Sustainable Energy Reviews*. 2011;15(8):3963-3979
[35] Vescovo R, Spagnoli E. High temperature orc systems. *Energy Procedia*. 2017;129:82-89
[36] Kim DK, Lee JS, Kim J, Kim MS, Kim MS. Parametric study and performance evaluation of an organic Rankine cycle (ORC) system using low-grade heat at temperatures below 80 C. *Applied energy*. 2017;189:55-65
[37] Tester JW, Anderson BJ, Batchelor AS, Blackwell DD, DiPippo R, Drake E, et al. The future of geothermal energy: Impact of enhanced geothermal systems (EGS) on the United States in the 21st century. *Massachusetts Institute of Technology*. 2006;209
[38] Di Pippo R. Geothermal power plants: principles, applications, case studies and environmental impact. Butterworth-Heinemann, 2012. 0123947871.
[39] Feng Y, Zhang Y, Li B, Yang J, Shi Y. Comparison between regenerative organic Rankine cycle (RORC) and basic organic Rankine cycle (BORC) based on thermoeconomic multi-objective optimization considering exergy efficiency and levelized energy cost (LEC). *Energy Conversion and Management*. 2015;96:58-71
[40] Calise F, Capuozzo C, Carotenuto A, Vanoli L. Thermoeconomic analysis and off-design performance of an organic Rankine cycle powered by medium-temperature heat sources. *Solar Energy*. 2014;103:595-609
[41] Qiu G. Selection of working fluids for micro-CHP systems with ORC. *Renewable Energy*. 2012;48:565-570
[42] Zhu S, Deng K, Qu S. Energy and exergy analyses of a bottoming Rankine cycle for engine exhaust heat recovery. *Energy*. 2013;58:448-457
[43] Tian H, Shu G, Wei H, Liang X, Liu L. Fluids and parameters optimization for the organic Rankine cycles (ORCs) used in exhaust heat recovery of Internal Combustion Engine (ICE). *Energy*. 2012;47(1):125-136

[44] Javan S, Mohamadi V, Ahmadi P, Hanafizadeh P. Fluid selection optimization of a combined cooling, heating and power (CCHP) system for residential applications. *Applied Thermal Engineering*. 2016;96:26-38

[45] Agudelo AF, García-Contreras R, Agudelo JR, Armas O. Potential for exhaust gas energy recovery in a diesel passenger car under European driving cycle. *Applied Energy*. 2016;174:201-212

[46] Dimitrova Z, Maréchal F. Energy integration study on a hybrid electric vehicle energy system, using process integration techniques. *Applied Thermal Engineering*. 2015;91:834-847

[47] Amicabile S, Lee J-I, Kum D. A comprehensive design methodology of organic Rankine cycles for the waste heat recovery of automotive heavy-duty diesel engines. *Applied Thermal Engineering*. 2015;87:574-585

[48] Yue C, You F, Huang Y. Thermal and economic analysis of an energy system of an ORC coupled with vehicle air conditioning. *International Journal of Refrigeration*. 2016;64:152-167

[49] Lemmens S. Cost engineering techniques and their applicability for cost estimation of organic Rankine cycle systems. *Energies*. 2016;9(7):485

[50] Di Battista D, Cipollone R, Villante C, Fornari C, Mauriello M. The potential of mixtures of pure fluids in ORC-based power units fed by exhaust gases in Internal Combustion Engines. *Energy Procedia*. 2016;101:1264-1271

[51] Cipollone R, Di Battista D, Bettoja F. Performances of an ORC power unit for Waste Heat Recovery on Heavy Duty Engine. *Energy Procedia*. 2017;129:770-777

[52] De Mena B, Vera D, Jurado F, Ortega M. Updraft gasifier and ORC system for high ash content biomass: A modelling and simulation study. *Fuel Processing Technology*. 2017;156:394-406

[53] Arena U, Di Gregorio F, De Troia G, Saponaro A. A techno-economic evaluation of a small-scale fluidized bed gasifier for solid recovered fuel. *Fuel Processing Technology*. 2015;131:69-77

[54] Kalina J. Integrated biomass gasification combined cycle distributed generation plant with reciprocating gas engine and ORC. *Applied Thermal Engineering*. 2011;31(14-15):2829-2840

[55] Vaja I, Gambarotta A. Internal combustion engine (ICE) bottoming with organic Rankine cycles (ORCs). *Energy*. 2010;35(2):1084-1093

[56] Tsai W, Chou Y. An overview of renewable energy utilization from municipal solid waste (MSW) incineration in Taiwan. *Renewable and Sustainable Energy Reviews*. 2006;10(5):491-502

[57] Bureau of Energy, Ministry of Economic Affair. Taiwan (ROC). Energy Statistics Handbook. 2016

[58] Chen F, Lu S-M, Tseng K-T, Lee S-C, Wang E. Assessment of renewable energy reserves in Taiwan. *Renewable and sustainable energy reviews*. 2010;14(9):2511-2528

[59] Kuo YT. ITRI. Industrial Technology Research Institute. Development of Biomass and Waste Energy in Taiwan. 2016

[60] [Bureau of Energy. Ministry of Economic Affairs. Taiwan (ROC). Renewable Energy Promotion Policies in Taiwan. 2015

[61] Costa M, La Villetta M, Massarotti N, Piazzullo D, Rocco V. Numerical analysis of a compression ignition engine powered in the dual-fuel mode with syngas and biodiesel. *Energy*. 2017;137:969-979

[62] Carrara S. Small-scale biomass power generation. 2010

[63] Jayah T, Aye L, Fuller RJ, Stewart D. Computer simulation of a downdraft wood gasifier for tea drying. *Biomass and Bioenergy*. 2003;25(4):459-469

[64] Ptasinski KJ, Prins MJ, Pierik A. Exergetic evaluation of biomass gasification. *Energy*. 2007;32(4):568-574

[65] Altafini CR, Wander PR, Barreto RM. Prediction of the working parameters of a wood waste gasifier through an equilibrium model. *Energy Conversion and Management*. 2003;44(17):2763-2777

[66] Costa M, La Villetta M, Massarotti N. Optimal tuning of a thermo-chemical equilibrium model for downdraft biomass gasifiers. *CHEMICAL ENGINEERING*. 2015;43

[67] Shashikantha B. PP and Parikh, PP, Development and performance analysis of a 15 kWe producer gas operated SI engine. *Proceedings of the Fourth National Meet on Biomass Gasification and Combustion, Mysore, India*. 1993;4:219-231

[68] Ramachandra A. Performance studies on a wood gas run IC engine. *Proceedings of Fourth National Meet on Biomass Gasification and Combustion, Mysore, India*. 1993;4(s 213)

[69] CLARKE ENERGY. Available at https://www.clarke-energy.com/. Last access: July, 27th 2018

[70] Hernandez JJ, Lapuerta M, Serrano C, Melgar A. Estimation of the laminar flame speed of producer gas from biomass gasification. *Energy & fuels*. 2005;19(5):2172-2178

[71] Woschni G. A universally applicable equation for the instantaneous heat transfer coefficient in the internal combustion engine. SAE Technical paper; 1967

[72] Heywood JB. Internal combustion engine fundamentals. 1988

[73] Obernberger I, Thek G. Combustion and gasification of solid biomass for heat and power production in Europe-state-of-the-art and relevant future developments. Conference Combustion and gasification of solid biomass for heat and power production in Europe-state-of-the-art and relevant future developments.

[74] EIA. U.S. Energy Information Administration. Available at: https://www.eia.gov/. Last access: July, 27th 2018

[75] Buonomano A, Calise F, Ferruzzi G, Vanoli L. A novel renewable polygeneration system for hospital buildings: Design, simulation and thermo-economic optimization. *Appl Therm Eng*. 2014;67(1):43-60

[76] GSE. Gestore Servizi Energetici. Available at: https://www.gse.it/. Last access: July 27th. 2018

[77] ECN. Overview of options for utilization of biomass ash. ECN-L--15--079. 2015;November

[78] ARERA. Autorità di Regolazione per Energia Reti a Ambiente. Available at: https://www.arera.it/it/index.htm#. Last access: July 27th. 2018